



Gravitational, erosional and depositional processes on volcanic ocean islands: Insights from the submarine morphology of Madeira Archipelago



Rui Quartau^{a,*}, Ricardo S. Ramalho^{b,c,d}, José Madeira^b, Rúben Santos^a,
Aurora Rodrigues^a, Cristina Roque^{b,e}, Gabriela Carrara^f, António Brum da Silveira^b

^a Divisão de Geologia Marinha, Instituto Hidrográfico – Marinha, 1200-615 Lisboa, Portugal

^b Instituto Dom Luiz, Faculdade de Ciências, Universidade de Lisboa, 1749-016 Lisboa, Portugal

^c School of Earth Sciences, University of Bristol, BS8 1RJ Bristol, UK

^d Lamont-Doherty Earth Observatory at Columbia University, 10964 New York, USA

^e Estrutura de Missão para a Extensão da Plataforma Continental, 2770-047 Paço de Arcos, Portugal

^f PROAMBIENTE Consortium, Emilia-Romagna High Technology Network, 40129 Bologna, Italy

ARTICLE INFO

Article history:

Received 20 March 2017

Received in revised form 31 October 2017

Accepted 1 November 2017

Available online xxxx

Editor: T.A. Mather

Keywords:

volcanic ocean islands

Madeira Archipelago

landslides and debris avalanches

gullies and channels

scour and wave fields

ABSTRACT

The submarine flanks of volcanic ocean islands are shaped by a variety of physical processes. Whilst volcanic constructional processes are relatively well understood, the gravitational, erosional and depositional processes that lead to the establishment of large submarine tributary systems are still poorly comprehended. Until recently, few studies have offered a comprehensive source-to-sink approach, linking subaerial morphology with near-shore shelf, slope and far-field abyssal features. In particular, few studies have addressed how different aspects of the subaerial part of the system (island height, climate, volcanic activity, wave regime, etc.) may influence submarine flank morphologies. We use multibeam bathymetric and backscatter mosaics of an entire archipelago – Madeira – to investigate the development of their submarine flanks. Crucially, this dataset extends from the nearshore to the deep sea, allowing a solid correlation between submarine morphologies with the physical and geological setting of the islands. In this study we also established a comparison with other island settings, which allowed us to further explore the wider implications of the observations. The submarine flanks of the Madeira Archipelago are deeply dissected by large landslides, most of which also affected the subaerial edifices. Below the shelf break, landslide chutes extend downslope forming poorly defined depositional lobes. Around the islands, a large tributary system composed of gullies and channels has formed where no significant rocky/ridge outcrops are present. In Madeira Island these were likely generated by turbidity currents that originated as hyperpycnal flows, whilst on Porto Santo and Desertas their origin is attributed to storm-induced offshore sediment transport. At the lower part of the flanks (–3000 to –4300 m), where seafloor gradients decrease to 0.5°–3°, several scour and sediment wave fields are present, with the former normally occurring upslope of the latter. Sediment waves are often associated with the depositional lobes of the landslides but also occur offshore poorly-developed tributary systems. Sediment wave fields and scours are mostly absent in areas where the tributary systems are well developed and/or are dominated by rocky outcrops. This suggests that scours and sediment wave fields are probably generated by turbidity currents, which experience hydraulic jumps where seafloor gradients are significantly reduced and where the currents become unconfined. The largest scours were found in areas without upslope channel systems and where wave fields are absent, and are also interpreted to have formed from unconfined turbidity currents. Our observations show that tributary systems are better developed in taller and rainy islands such as Madeira. On low-lying and dry islands such as Porto Santo and Desertas, tributary systems are poorly developed with unconfined turbidite currents favouring the development of scours and sediment wave fields. These observations provide a more comprehensive understanding of which factors control

* Corresponding author at: Divisão de Geologia Marinha, Instituto Hidrográfico – Marinha, 1200-615 Lisboa, Portugal.

E-mail address: rui.quartau@hidrografico.pt (R. Quartau).

the gravitational, erosional, and depositional features shaping the submarine flanks of volcanic ocean islands.

© 2017 Elsevier B.V. All rights reserved.

1. Introduction

The main volume of volcanic islands lies hidden beneath the sea and consequently their submarine flanks are far less studied than their accessible subaerial parts. The study of the submarine pedestals of volcanic islands is of great significance, because it can significantly improve our knowledge of island evolution, particularly if integrated with information on the development of subaerial edifices (Moore et al., 1989; Masson et al., 2002; Leat et al., 2010; Quartau and Mitchell, 2013; Saint-Ange et al., 2013; Quartau et al., 2015a). The advent of modern seafloor surveys during the 1980s, with sidescan and multibeam sonars, allowed the discovery of large-scale landslides (Moore et al., 1989; Masson et al., 2002), canyons and turbidite systems (Krastel et al., 2001; Sisavath et al., 2011), and sediment wave (Wynn et al., 2000a; Hoffmann et al., 2008) and scour fields (Hoffmann et al., 2011). Despite the vast range of published works, however, few comprehensive source-to-sink studies on ocean island volcanoes have focused on the development of their submarine flanks. Moreover, whether based on drilling (e.g., Schmincke and Sumita, 1998) or on the characterization of their submarine morphologies, most studies focus on a single island (e.g., Saint-Ange et al., 2013) or on a single process (e.g., Hunt et al., 2014). Consequently, works rarely relate subaerial conditions and shelf processes with the development of deeper submarine morphologies.

In this study, we make use of novel multibeam bathymetric and backscatter mosaics of an entire archipelago – which crucially extend from the nearshore to the abyssal plains – to gain a comprehensive insight on the origins of several gravitational, erosional and depositional features shaping the submarine flanks of volcanic islands. Furthermore, a correlation with the diverse physiographic conditions and geological evolution of each of the islands, allowed us to understand how these characteristics conditioned their present-day submarine flank morphologies. The case study of Madeira Archipelago is therefore particularly elucidative providing a unique insight onto the evolution of the submarine flanks of reefless oceanic volcanoes.

2. Regional setting

Madeira Archipelago is located in the NE Atlantic, ~1000 km SW of the Iberian Peninsula (Fig. 1). It comprises the islands of Madeira (737 km²), Porto Santo (42 km²), and Desertas (13 km²). The island edifices are the result of intra-plate volcanism on the slow-moving Nubian plate, leading to a hotspot track extending to the NE (Geldmacher et al., 2000). Although administratively included in Madeira Archipelago, the Selvagens Islands (~3 km²) constitute, from the geological point of view, a distinct archipelago and will be presented in a future study.

Madeira is the youngest island, with volcanism extending from >7 Ma to the Holocene (Geldmacher et al., 2000; Mata et al., 2013; Ramalho et al., 2015). Subaerial Madeira extends 58 km in the WNW–ESE direction and has an average width of 15 km (annotation 1 in Fig. 2). The island is an elongated shield volcano, which despite being highly dissected, is largely above 1200 m, reaching a maximum elevation of 1862 m at Pico Ruivo. This configuration of the island constitutes a barrier to the dominant NE trade winds, causing higher precipitation in the north-facing slopes (Prada et al., 2005). Notwithstanding this asymmetry, Madeira has a well-developed and deeply incised subaerial drainage system on both

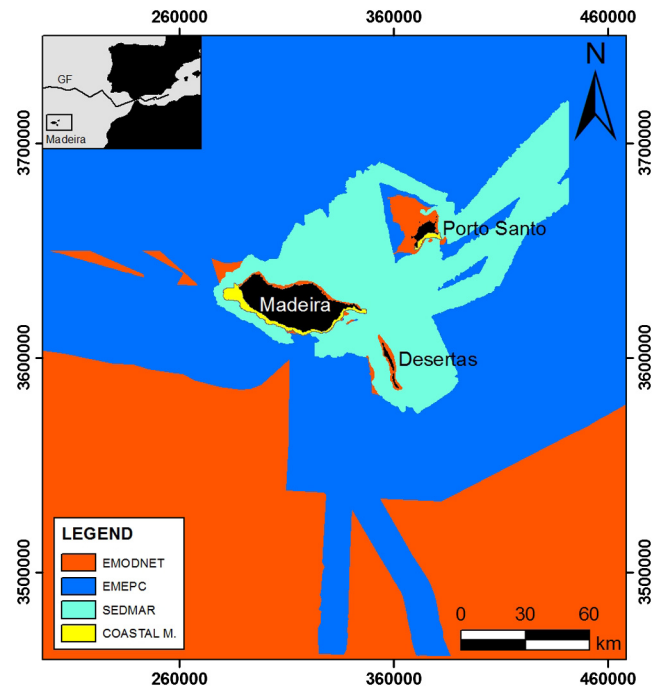


Fig. 1. Upper-right inset shows the location of Madeira Archipelago (GF – Gloria Fault) and main panel shows the sources of the different bathymetric datasets. Black areas represent the continental and island landmasses. Coloured areas represent the bathymetric sources: yellow, data from coastal management projects; light-blue, from SEDMAR; dark blue, from EMEPC; and orange, from EMODnet projects. This map and the following have UTM 28N coordinate system. (For interpretation of the references to colour in this figure legend, the reader is referred to the web version of this article.)

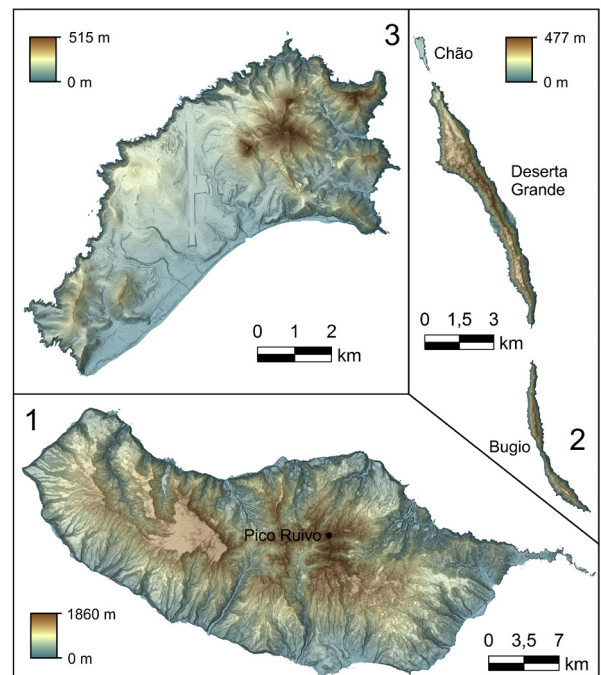


Fig. 2. Shaded relief images of the subaerial topography of the islands of Madeira (1), Porto Santo (2) and Desertas (3). Data is from Direção de Serviços de Informação Geográfica e Cadastro do Governo Regional da Madeira.

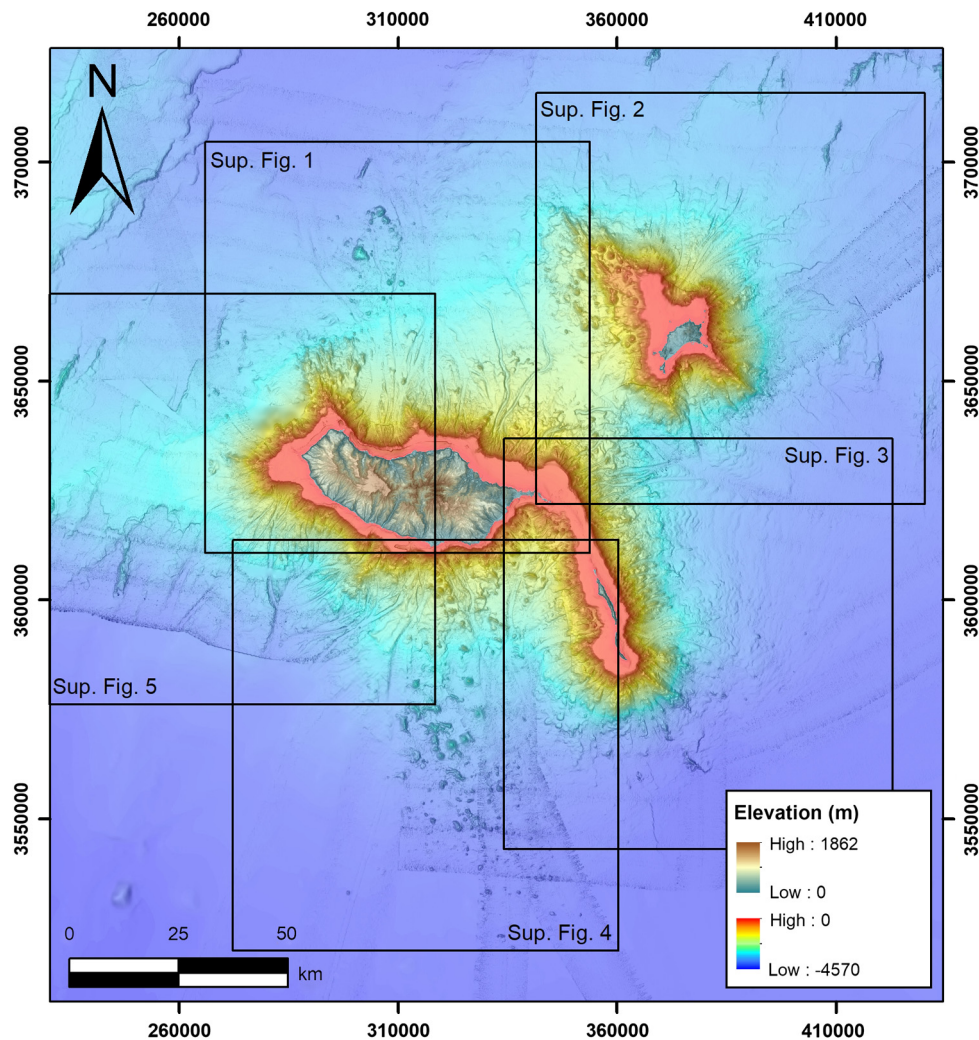


Fig. 3. Shaded relief image derived from the bathymetric compilation. Squares locate high resolution sub-sets of this bathymetric compilation that can be found in the supplementary material section.

flanks, mostly oriented N–S, descending on average from 1200 m to sea level in only 6 km. The annual precipitation on Madeira varies from 600–800 mm on the south coast to 1500–2000 mm on the north, reaching 3000 mm in the higher ranges (Baioni, 2011). Rainfall is often temporally concentrated making the island very prone to flash floods and subaerial landslides (Baioni, 2011). During the flash-flood of 20th February 2010, rainfall attained 500 mm in a single day and the volume of solid discharge deposited in the Funchal urban area reached $\sim 250,000 \text{ m}^3$ (Lira et al., 2013).

The Madeira-Desertas system is considered to be the expression of two arms of a volcanic rift intersecting at an angle of $\sim 110^\circ$ and surrounded by the 200 m isobath (Klügel et al., 2009). The Desertas Islands (from north to south: Ilhéu Chão, Deserta Grande and Bugio) correspond to the 50 km-long NNW–SSE trending arm, although their subaerial expression is now only 22 km long (annotation 2 in Fig. 2). Effectively, these islands are presently reduced to very narrow ridges (< 2 km), featuring subaerial aspect ratios (height/width) between 0.2 and 0.6, clearly the result of strong wave erosion and landsliding. Volcanism leading to the formation of Desertas shows similarities with Madeira's, although its volcanic activity ceased 1.9 Ma ago (Schwarz et al., 2005).

Porto Santo is separated from the Madeira-Desertas system by a 30 km wide and 2500 m deep channel (annotation 3 in Fig. 2 and Fig. 3). It is a much older island (with volcanic activity restricted to 14–10 Ma), being significantly eroded and lying below

517 m of elevation (Schmidt and Schmincke, 2002). It has an average annual precipitation < 400 mm, typical of a semi-arid climate. Streams have an ephemeral character and only flow after heavy rainfall (Ferreira and Cunha, 1984).

3. Data and methods

The comprehensive multibeam mapping around Madeira Archipelago was performed by the Portuguese Hydrographic Institute (IH) under the programs EMEPC (Estrutura de Missão para a Extensão da Plataforma Continental) and SEDMAR (Sedimentary environment of the Madeira Archipelago). The intermediate and deeper bathymetry was acquired by IH, between 2005 and 2014, using the Kongsberg EM710 and EM120 multibeam echo-sounders aboard R/Vs “Almirante Gago Coutinho” and “D. Carlos I”. Multibeam bathymetry of the southern shelves of Madeira and Porto Santo was also acquired by IH during coastal management projects, between 2003 and 2008, with the Kongsberg EM3000 and EM3002 echo-sounders onboard survey launches. Multibeam surveys were mostly DGPS-positioned and processed using Caris software Hips & Sips. Corrections were done by manual editing of data before 2011 and with CUBE (Combined Uncertainty and Bathymetric Estimator, Calder and Mayer, 2003) after 2011. Bathymetric data acquired above -200 m included tide corrections based on published tidal charts. High-resolution digital elevation models were produced with cell-size

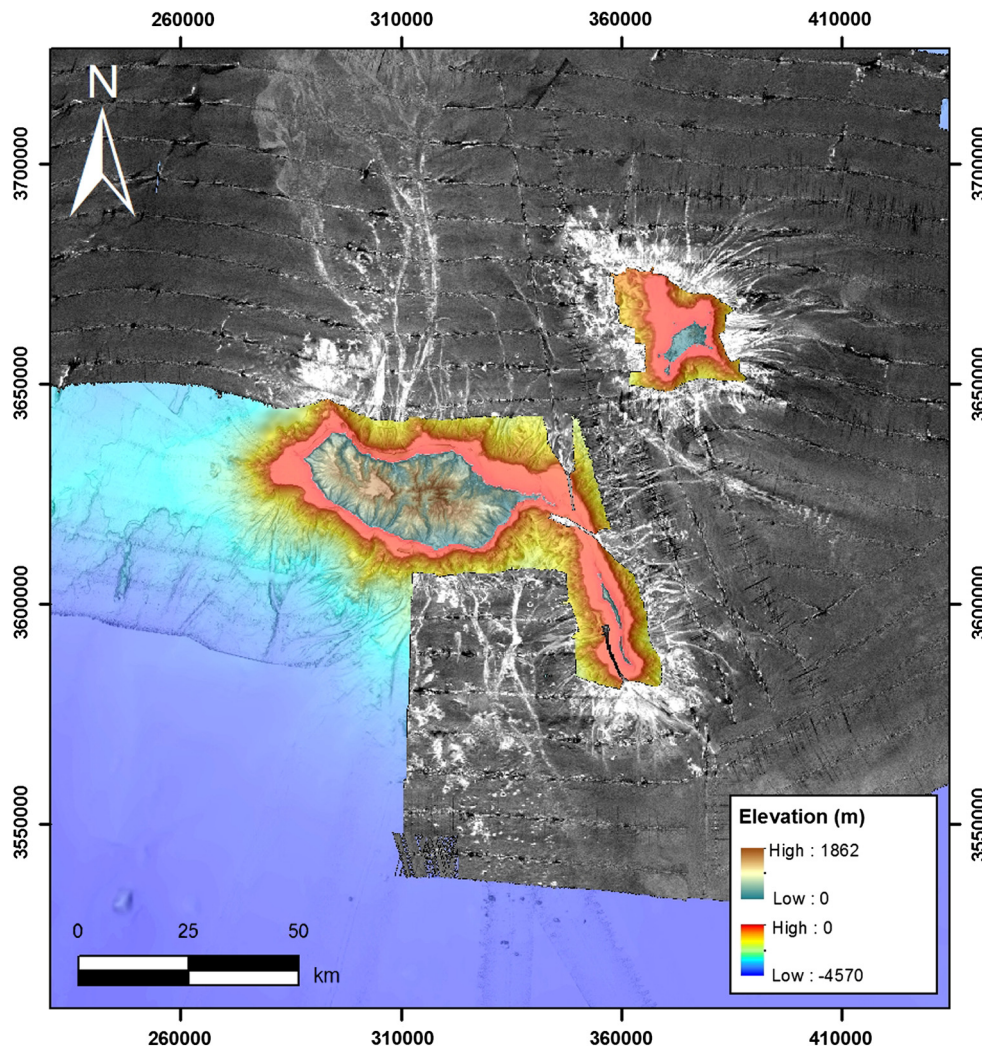


Fig. 4. Acoustic backscatter mosaic with low values in black and high values in white (-70 dB to 10 dB).

varying from 2 m in areas < -100 m to 250 m at -4500 m (Fig. 3). Radiometric and geometric corrections were also applied to the raw data with the Geocoder algorithm implemented in the software Fledermaus Pro to build backscatter strength mosaics (Fig. 4). Single-beam bathymetry (grid-size of $\sim 230 \times \sim 190$ m), from the European Marine Observation and Data Network (EMODnet) project filled gaps between multibeam datasets.

The multichannel seismic reflection profile Torem060 was acquired by IFREMER during the TORE-MADÈRE cruise (25th September–20th October 2001), using a six-channel streamer at 5 m depth and two GI airguns ($105/105$ and $45/45$ cu in.) at a surface speed of 10 knots (Cornen et al., 2003). The seismic line was processed using a spherical divergence correction, a band pass filter, and stacking of the six channels to improve the signal/noise ratio.

4. Results

The features identified on the multibeam bathymetry, backscatter and seismic reflection datasets allowed mapping the submarine flanks of the archipelago in detail, from the coastline down to -4500 m. Seafloor interpretation was divided into gravitational (headwall scars of landslides and respective debris avalanches), erosive (gullies, channels and scour fields), and depositional morphologies (sediment wave fields).

4.1. Large landslides

4.1.1. NW Madeira

This landslide exhibits the largest headwall scar (~ 22 km in length) of all the identified shelf edge failures, and is mimicked by an adjacent concave coastline (annotation 1 in Fig. 5 and Table 1). It was previously identified based on onshore geomorphology and named “São Vicente landslide” (Brum da Silveira et al., 2010a). The scar is incised by small gullies (black lines in Fig. 5), a few hundred-metres wide and up to 10 km in length, commonly having a V-shaped section. They are commonly organized in parallel networks, slightly converging downslope into three wider and flat-bottomed channels without a marked headwall. The gullies are restricted to the chute area and their transition into the channels occurs at ~ -2000 m, corresponding to an abrupt change of gradient. The three main channels are each around 60 km in length, with widths varying from 1 to 5 km. They divert inside a somewhat lobate area with an irregular seafloor punctuated by some large blocks between -3000 m and -4000 m. The blocks are irregular, with varying sizes, from a few hundred metres to a few kilometres in diameter. The largest is 3 km in diameter and rises 0.6 km above the surrounding seafloor. The seismic line Torem060 (Fig. 6) crosses debris avalanche n° 1 and shows an irregular and sometimes hyperbolic seafloor reflection between shots 2350 and 3000 (Fig. 6). This irregular surface corresponds in depth to a single chaotic seismic unit (~ 250 ms thick), interpreted as deposits of

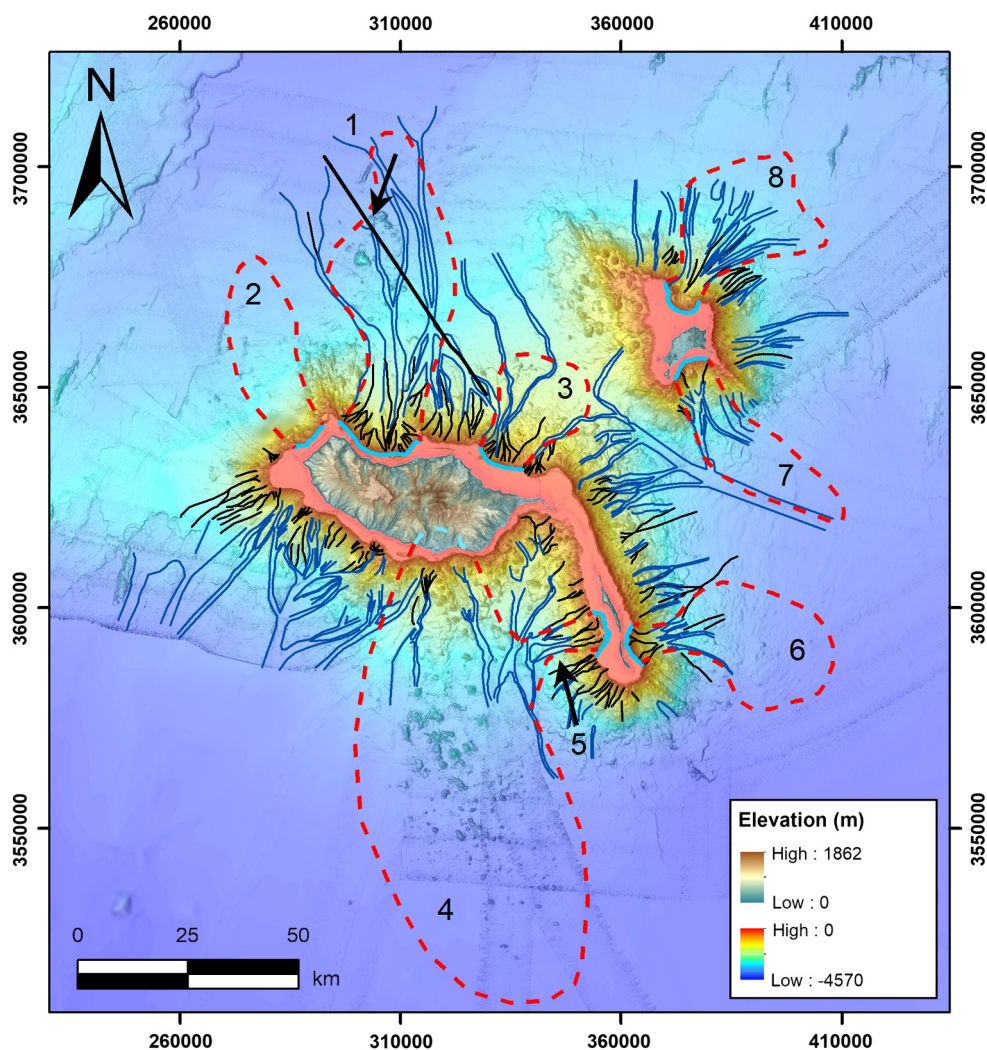


Fig. 5. Interpreted submarine topography: light blue lines represent the headwall scars of the landslides, black lines represent the gullies, dark blue lines represent the channels and dotted red lines represent the outline of the depositional lobes of the landslides' debris avalanches. Annotations 1 to 8 correspond to the numbering of the different landslides referred in the text. Arrow over lobe 1 locates shot 2350 of seismic profile Torem060. The other arrow SW of Desertas points to the landslide area no. 5. (For interpretation of the references to colour in this figure legend, the reader is referred to the web version of this article.)

the debris avalanche n° 1. Around shot 2350, this unit is abruptly replaced by a well-stratified unit along a plane dipping $\sim 20^\circ$ to the NW. The three main channels inside debris avalanche n° 1 widen and give way to a braided channel system only perceptible in the backscatter imagery (Fig. 4). High backscatter values suggest the channel filling by coarser sediments, dissecting normal pelagic sedimentation (seen in the seismic line as well-defined and rhythmic reflections between shots 2000 and 2350).

4.1.2. NNW Madeira

This landslide is inferred by the slightly concave configuration of the shelf edge, featuring a ~ 8 km wide headwall scar and downslope by a somewhat lobate debris avalanche deposit (annotation 2 in Fig. 5 and Table 1). The surface of this deposit is dissected by scour fields from 12 to 25 km of the scar, evolving to a sediment wave field that extends up to 43 km offshore (see sections 4.3 and 4.4 and Fig. 7).

4.1.3. NE Madeira

This landslide is inferred by the concave configuration of the shelf edge, which features a ~ 20 km wide headwall scar (annotation 3 in Fig. 5 and Table 1). Onshore, the coastline mimics this concave configuration, exhibiting steep cliffs up to 700 m high.

Table 1

Approximate dimensions of the debris avalanches of large landslides in Madeira Archipelago.

Number	Name	Area (km ²)	Length (km)	Width (km)	Type
1	NW Madeira	1350	85	25	Debris Flow
2	NNW Madeira	550	47	15	Debris Flow
3	NE Madeira	500	35	20	Debris Flow
4	SE Madeira	4000	110	45	Debris Flow
5	SW Desertas	100	20	5	Debris Flow
6	SE Desertas	780	45	20	Debris Flow
7	S Porto Santo	570	50	12	Debris Flow
8	N Porto Santo	700	42	23	Debris Flow

This landslide had been previously proposed by Geldmacher et al. (2000) and named “Porto da Cruz landslide” by Brum da Silveira et al. (2010a). The shelf break is incised by small gullies that form three main channels further offshore.

4.1.4. SE Madeira

This landslide is inferred by the hummocky seafloor morphology that extends ~ 100 km from the shelf break (annotation 4 in Fig. 5 and Table 1). Some of these reliefs correspond to a NNW–

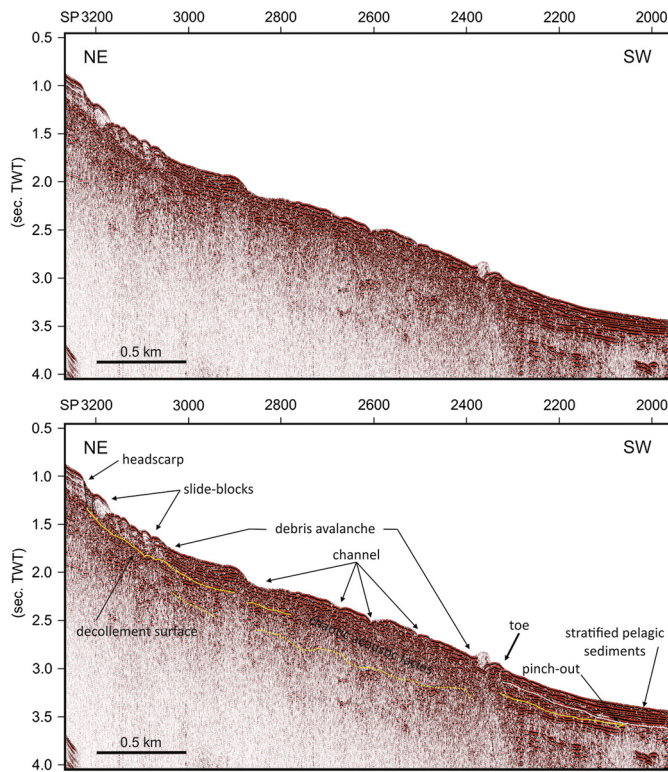


Fig. 6. Seismic profile Torem060 crossing the NE Madeira sector and showing a downslope gradation from almost undeformed slide-blocks to a debris avalanche characterized by chaotic facies. The central and thicker part of the debris avalanche is incised by channels. The sediments of the toe area seem to be slightly folded suggesting the occurrence of some compressional deformation when the debris avalanche stopped. A chaotic facies body with pinch-out and overlapped by stratified pelagic sediments can be seen in the SW sector of the seismic line suggesting the presence of a past debris flow.

SSE, ~60 km long alignment of submarine volcanic cones, named the “Funchal Volcanic Ridge” by Klügel and Klein (2006). However, within this ~100 km strip, several features exhibit irregular shapes, typical of blocks from a large debris avalanche deposit. Onshore, the morphology corresponds to a wide amphitheatre. This feature has been interpreted as a subaerial scar of a flank collapse (named “Funchal landslide”), which has been covered by recent volcanism of the Upper Volcanic Complex (Brum da Silveira et al., 2010b; Ramalho et al., 2015). The shelf break is incised by small V-shaped gullies, a few hundred-metres wide and up to 2–3 km in length. These are generally organized in sub-parallel networks, slightly converging downslope into several wider and flat-bottomed channels without a marked headwall. This channel system is diverted around seafloor irregularities (cones and blocks) and ends gradually around 30–60 km from the shelf break.

4.1.5. SW Desertas

This landslide is inferred from a ~10 km wide concave incision of the shelf break, roughly mimicked by the arcuate coastline of the adjacent Deserta Grande (annotation 5 in Fig. 5 and Table 1). Downslope of the headwall scar, there is a mid-slope bench at ~400 m, where three U-shaped, 1–2 km-wide channels originate. These channels run perpendicular to the slope (WSW-ENE) for ~19 km where they merge into a larger channel oriented roughly N–S coming from SE Madeira.

4.1.6. SE Desertas

This landslide is also inferred from the concave morphology of the shelf break and by the arcuate coastline of Bugio (annotation

6 in Fig. 5 and Table 1). The headwall scar is ~9 km wide, adjacent to a wide chute area incised by small gullies. At around ~2000 m and 6 km from the shelf edge, the gullies stem into a series of small parallel channels less than 1 km wide, which incise the seafloor up to 20 km offshore. At the end of the channels there are some scours perpendicular to the channels’ direction, followed by a large wave field (see sections 4.3 and 4.4 and Fig. 7). The entire system (channel, scours and wave fields) exhibits a somewhat lobate shape.

4.1.7. S Porto Santo

This landslide is also inferred by the concave shelf break with a ~10 km wide headwall scar, backed by a coastline mimicking the arcuate shelf edge (annotation 7 in Fig. 5 and Table 1). Below the shelf break, there is a wide chute area of 5–6 km in length stemming into a system of channels at its base. The westernmost channel discharges on a larger channel that collects sediments from other smaller channels dissecting the NE slopes of Desertas. This main channel marks the SW border of a lobate feature containing the landslide chute, channels, scours, and wave fields (Figs. 5 and 7).

4.1.8. N Porto Santo

This landslide has a very arcuate headwall scar, ~9 km wide that gives away downslope to a series of divergent gullies and channels (annotation 8 in Fig. 5 and Table 1). The areas between the channels are extremely scoured whilst the channels are filled with rhythmic waves (see sections 4.3 and 4.4 and Fig. 7).

4.2. Gullies and channels

The submarine flanks of Madeira, Desertas, and Porto Santo are extensively incised by numerous gullies and channels (Fig. 5). These can be easily distinguished in the backscatter mosaic, showing linear features with high backscatter values (corresponding to coarser sediments) relative to the surrounding environment (Fig. 4). The shelf edge around the islands often exhibits small headscars that stem into one or more gullies, suggesting continuous headwall erosion and transport downslope. The gullies are located on the steepest upper submarine flanks of the islands (gradients >15°); they are V-shaped in cross-section and can be up to 5–10 km in length and a few hundred metres wide. They can either be parallel or dendritic, but the latter dominates, normally converging into U-shaped channels. The channels develop normally at gradients lower than 15°, commonly with parallel to dendritic pattern. The dendritic channels often converge downslope into a larger main channel, whilst the parallel ones remain with that configuration or in some cases diverge, forming fan-shaped systems such as to the N of Porto Santo. The smaller and upper channels are ~500 m-wide, but the lower and wider ones can reach 5 km in width and extend up to 60–70 km from the shelf break (as in NW Madeira). These channel systems are well developed on the northern and southern submarine flanks of Madeira, and in the area between Desertas and Porto Santo. They are less developed on the W and E slopes of Desertas and the NE, SE and E of Porto Santo. They are absent on the NNW Madeira and in the NW, W, and SW slopes of Porto Santo. In the NW and SE of Madeira, the channels are deflected by large irregularities on the seafloor. SW of Madeira, the channel system probably extends much further than we can disclose (~35 km), but the lack of multibeam bathymetry in this area prevented mapping the entire system.

4.3. Sediment wave fields

Sediment wave fields are found East of Desertas, SE and NE of Porto Santo and, NNW of Madeira (Fig. 7). Their wave length generally increases with increasing water depths (Fig. 8 and Table 2).

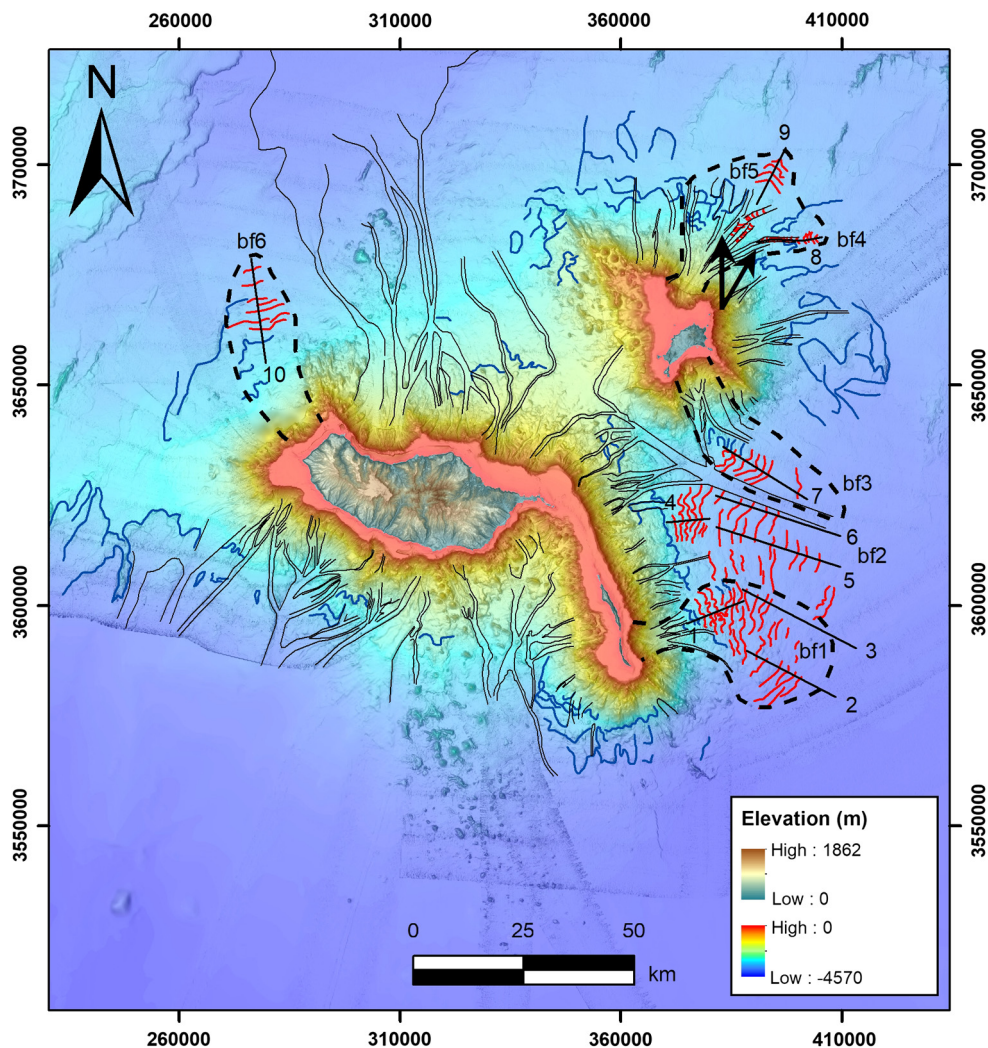


Fig. 7. Interpreted submarine topography: black lines represent the channels, red lines represent the wave crests of the bedforms, annotation with prefix bf* represent the defined bedform fields listed in Table 2, arrows point to wave fields inside channels, black straight lines and numbers next to them locate the topographic profiles of Fig. 8, dark blue lines represent the headwall of the scours, and dotted black lines represent the outline of the depositional lobes of the interpreted landslides’ debris avalanches. (For interpretation of the references to colour in this figure legend, the reader is referred to the web version of this article.)

Table 2 Synthesis of the main morphological features of the different sediment wave fields around the islands of Madeira, Porto Santo and Desertas.							
	Wave length (m)	Wave height (m)	Seafloor gradient (°)	Depth range (m)	Cross-section	Wave crests	Comments
bf1_shallow	1350–1700	25–35	3.7	3000–3800	downslope asymmetrical	Very sinuous	inside debris avalanche deposits
bf1_deep	800–3300	9–42	0.6–2	3800–4300	upslope asymmetrical	Less sinuous	inside debris avalanche deposits
bf2_shallow	1500–2000	16–32	2.9	3000–3600	upslope asymmetrical	Very sinuous	seaward of the end of channels
bf2_deep	1900–4800	9–42	0.6–1.3	3600–4300	upslope asymmetrical	Less sinuous	seaward of the end of channels
bf3	1100–4000	11–94	0.9–2.4	3400–4000	downslope asymmetrical	Less sinuous	inside debris avalanche deposits
bf4	600–1200	2–17	1.2–1.9	3000–3500	both	crescentic downslope	inside channels
bf5	1300–2400	4–16	1.4	3300–3600	downslope asymmetrical	crescentic upslope	inside debris avalanche deposits
bf6	1200–3000	9–30	0.8–1.9	3400–3700	upslope asymmetrical	Less sinuous	inside debris avalanche deposits

Descriptions of bedform cross-section geometry and planform crest shape are based on Symons et al. (2016) classification.

4.3.1. East of Desertas

At Desertas, sediment wave fields are present on their eastern slopes below –3000 m and where gradients are <5° (Figs. 7 and 8). At this depth, the channels that incise the slope of Desertas gradually disappear and give way to scours. Thus, the scours constitute a gradual transition to the wave fields, making them difficult to separate in some places. Immediately below the transitional area (at –3000 to –3800 m and gradients 2.9°–3.7°), the bed-

forms exhibit wave lengths of 1350–2000 m and wave heights of 150–350 m. Below –3800 m and, down to –4300 m, seafloor gradients decrease from 2° to 0.6° and the bedforms become widely spaced (1900–4200 m) and taller (500–1400 m). Generally, these bedforms show sinuous and often undulating crestlines in plan-view and are upslope asymmetrical in cross-section (according to the classification of Symons et al., 2016). The stoss sides slope shoreward, and are normally less steep and shorter than the lee sides that slope seaward. However, examples of downslope asymmetrical cross-sections are also found showing stoss sides sloping seaward. There are mainly two fields of bedforms, one in front of

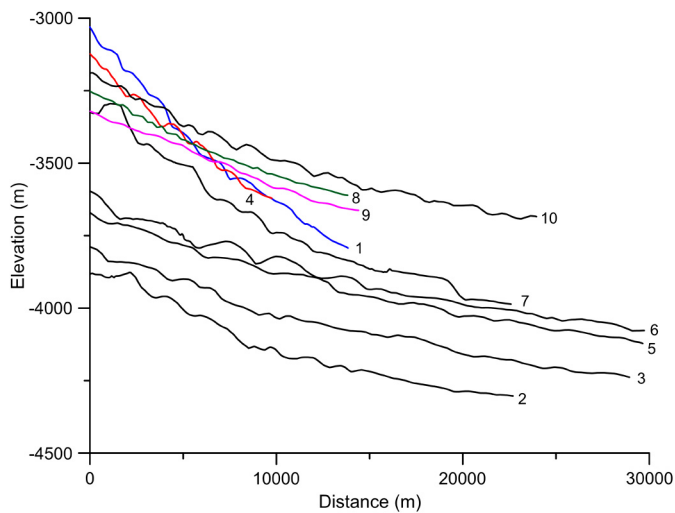


Fig. 8. Topographic profiles of the sedimentary wave-fields.

the eastern landslide headwall scar (bf1 in Fig. 7 and profiles 1, 2 and 3 in Fig. 8) and another (bf2 in Fig. 7 and profiles 5 and 6 in Fig. 8) that extends downslope at the end of a series of parallel channels (Fig. 5).

4.3.2. SE Porto Santo

SE of Porto Santo, the wave fields occur on top of a volcanoclastic bulge with lobate-shape (bf3 in Fig. 7 and profile 7 in Fig. 8). The bedforms also occur downslope of scours, showing a transition from well-developed scours to more rhythmic bedforms. The bedforms develop between -3400 m and -4000 m at seafloor gradients $<2.4^\circ$. Generally, these bedforms show less sinuous crestlines in plan-view and are downslope asymmetrical in cross-section.

4.3.3. NE Porto Santo

NE of Porto Santo bedforms develop in two settings (Figs. 7 and 8). Some bedforms can be found inside channels (indicated by arrows and bf4 in Fig. 7 and profile 8 in Fig. 8) and others (bf5 in Fig. 7 and profile 9 in Fig. 8) on top of a volcanoclastic bulge with a lobate-shape. In both cases there are no scours upslope of the bedforms.

On top of the bulge, bedforms occur at -3300 m to -3600 m, on seafloor gradients of 1.4° , with wave lengths of 1300 – 2400 m and wave heights of 4 – 16 m. They show somewhat crescent upslope crestlines in plan-view and are downslope asymmetrical in cross-section.

Inside the channels, bedforms occur at -3000 m to -3500 m, in seafloor gradients of 1.2° – 1.9° , with wave lengths of 600 – 2000 m and wave heights of 2 – 17 m. They show crescent downslope crests in plan-view and have both downslope and upslope asymmetry in cross-section. On the shallower sections of the channels, bedforms probably also exist but the resolution of the bathymetry does not allow the identification of these features.

4.3.4. NNW Madeira

Here the bedforms develop on top of a lobate body, stemming from an arcuate scar (bf 6 in Fig. 7 and profile 10 in Fig. 8) at the shelf edge. The bedforms occur between -3400 m to -3700 m on a seafloor with gradients between 0.8 – 1.9° . Upslope, they are bounded by a series of sinuous scours that can extend up to -3000 m. The bedforms show an almost linear shape in plan view and are upslope asymmetrical in cross-section.

4.4. Scours

The term scour is used here to denote erosional bedforms, often characterized by enclosed depressions (Wynn et al., 2002; Symons et al., 2016). They were identified in the bathymetry as headwall scars mostly transverse to the main slope, being generally deeper downslope of the headwall. Being abundant on the lower slopes of Madeira Archipelago (Fig. 7), these features were found in four different settings: (1) between the channel systems and the wave fields (e.g., E of Desertas and SE of Porto Santo); (2) at the end of the gully/channel systems but without offshore wave fields (e.g., N and E of Porto Santo and around the southern tip of Desertas), (3) where no channel system exists (e.g., NW of Porto Santo and NNW and SSW of Madeira, the latter displaying the largest scours); and; (4) on ridges between the channels (e.g., S and NE of Madeira).

These structures display mostly linear to sinuous shapes in plan-view. The sinuous ones are commonly rectangular or U-shaped in plan-view and seem to be formed by coalescing individual scours. The coalescing scours feature headwalls up to 10 – 30 km in width, 20 km in length and 200 m deep (e.g., SW of Madeira). Individual scours can be less than 1 km in width and length, and 10 – 20 m deep. Smaller scours were not mapped because they fall beyond the resolution of bathymetry. All scours occur within the same depth range (-3000 to -4300 m) and seafloor gradients (0.5° – 3°) as the wave fields.

5. Discussion

5.1. Large landslides

It has been proposed that the occurrence of large landslides (involving volumes in excess of 1 km^3 or areas over a few hundreds of km^2 , Siebert, 1984; Paris et al., 2018) is controlled by edifice elevation and topography of individual islands (Mitchell, 2003). Here we explore our observations of large landslides in Madeira Archipelago and set these in the context of other volcanic islands.

Eight large landslides were identified and most of them exhibit: (i) well-defined amphitheatres at their source regions; (ii) well defined chute areas of up to 10 km in length and 2 km in height; and (iii) debris avalanche fields with somewhat lobate shapes, albeit being significantly incised by channel systems. Some of these slide deposits still exhibit hummocky morphologies with mega blocks up to 3 km wide (NW and SE Madeira). Additionally, with the exception of the landslides inferred SE of Madeira and N of Porto Santo, all sites exhibit concave coastlines mimicking the arcuate shelf break scars. It must be noted, however, that the SE Madeira landslide probably also created an arcuate coastline – corresponding to the “Funchal amphitheatre” – but the area has subsequently been covered by post-collapse volcanism (Brum da Silveira et al., 2010a). The western lateral ramp of this landslide probably corresponds to the erosional unconformity observed at Cabo Girão between the Middle and the Upper Volcanic Complexes and thus it must pre-date the Lombos Unit of the Upper Volcanic Complex (~ 1.8 Ma, Brum da Silveira et al., 2010a). Nevertheless, the size and extent of the debris avalanche deposits (larger than the NW landslide) suggest a greater volume than the one implied by Brum da Silveira et al. (2010a). Thus, we do not exclude the possibility that this avalanche debris corresponds to an earlier and even larger event than the “Funchal landslide”. Otherwise the Funchal submarine volcanic ridge (<3 Ma, according to Geldmacher et al., 2006) would have been buried by the debris avalanche flow.

The presence of arcuate shorelines is a testimony that these major landslides most likely affected the subaerial and submarine portions of the volcanic edifices. Subsequently, the incision of the island flanks by waves during Quaternary glacio-eustatic sea level-oscillations produced the observed shelves (>1 km wide). In the

Azores, such wide shelves were produced over several hundreds of thousands of years (Quartau et al., 2010; Quartau et al., 2012; Quartau et al., 2014; Quartau et al., 2015b, 2016). Therefore, we suspect that all these major landslides are also at least several hundreds of thousands of years, since they show at least one of the following features: (1) well-developed channel systems in front of their chutes, incising the debris avalanche deposits; (2) relatively wide-shelves (>1 km) in front of the arcuate coastlines, and (3) filling by post-collapse volcanism, dating at least several hundreds of thousands of years (Brum da Silveira et al., 2010a; 2010b).

Madeira Island landslides are the largest of the archipelago (Table 1) and have dimensions of the same order of magnitude of those reported for the Canaries (Table 1 at Acosta et al., 2003). They are also similar to the landslides in Hawaii with the exception of the three largest ones (North Kauai, Nuanu at Oahu, and Wailau at Molokai), which are three to six times larger than the SE Madeira landslide (Table 1 at Moore et al., 1989). Landslides at Porto Santo and Desertas are, however, smaller than the ones at Madeira. Thus, this study also suggests that there is a clear relationship between landslide dimension and island sizes/topography, as it happens in other archipelagos. Mitchell (2003) also suggested that landslides are more common in edifices taller than 2500 m. Landslides with dimensions similar to the smaller ones at Hawaii and Canaries, however, also occur at Porto Santo and Desertas, which are islands that clearly never reached such heights. Further studies are therefore needed to understand exactly which conditions favored these catastrophic events at Madeira Archipelago.

5.2. Gullies and channels

The submarine network of gullies and channels is very well developed N and S of Madeira and between Desertas and Porto Santo where channels from both islands converge into a larger main channel. The parallel gullies (V-shaped) in the upper slope converge downslope into wider and flat-bottomed channelized features (U-shaped). In turn, these structures also tend to convergers into one or more larger channels, with transition from gullies to channels occurring at gradients smaller than 15°. The increase in width downslope could be the result of lateral erosion predominating over vertical incision. This and the decrease of gradients could promote deceleration of the flows and consequent sediment infilling of the seafloor creating the U-shaped drainage system. The pathways of these features are strongly influenced by the presence of rocky outcrops. Consequently, this tributary system is absent where protruding rocky outcrops and bulge areas are abundant such as to the W of Porto Santo and NNW of Madeira. It is also poorly developed to the NE of Madeira. To the NW and SE of Madeira, the channels, albeit being well-developed, are diverted around obstacles such as the volcanic cones and collapsed blocks.

According to Krastel et al. (2001), submarine drainage in Gran Canaria and Tenerife (Canaries) was initiated by flash floods that crossed the island shelf as hyperpycnal flows. When these flows reached the steep upper slopes of the islands, they accelerated and carved proto-gullies aligned with the subaerial drainage. Other studies provided similar interpretations for the formation of submarine drainage at Tenerife, El Hierro (Mitchell et al., 2003), La Gomera (Llanes et al., 2009) and Réunion Islands (Mazuel et al., 2016). When volcanic activity wanes, abrasion and widening of the insular shelf prevents the direct stream discharge on the insular slope and the development of the submarine drainage diminishes (Mitchell et al., 2003). However, the submarine drainage once initiated is probably continued by exceptional erosive sediment flows coming from onshore, and reaching the upper slopes of the islands and/or by failures of the gullies' walls (where gradients reach >15°). In either case, downslope eroding flows such as turbidites,

are probably responsible for the development of the submarine drainage.

The three main factors controlling sediment supply and transport offshore volcanic islands are, in decreasing importance, volcanic activity, climate and sea-level changes (Krastel et al., 2001). Turbidites are more likely formed during flank collapses and syn-eruptive mass flows (e.g., pyroclastic flows, lahars) (Manville et al., 2009). Hence, sedimentation rates in the slope apron are likely to be highest during phases of high volcanic activity and decrease during non-eruptive phases (Carey and Schneider, 2011). When volcanic activity wanes, subaerial erosion increases and gullies evolve into streams bringing terrigenous sediments to the shelf (Saint-Ange et al., 2013). Steeper slopes and high precipitation rates result in stronger erosion that generates hyperpycnal flows, which are capable of transporting riverine sediments across the shelf onto the edge (Mazuel et al., 2016). An additional important source of material is the reworking of unconsolidated volcanoclastic material previously deposited in the marine environment, termed 'secondary volcanoclastic turbidites' (Carey and Schneider, 2011). Storm waves are able to transport large amounts of nearshore sediments into the shelf edge and upper slopes of the islands (Tsutsui et al., 1987). The initiation of submarine gravity flows by storm waves is recognised on continental margins where narrow shelves exist and canyon heads incise most of the shelf (e.g. at La Jolla and Monterey canyons, Piper and Normark, 2009). Sediments deposited progressively nearby the canyon heads or the outer shelf during floods can become unstable and fail when a loading threshold is reached (Mazuel et al., 2016). Shelf storage also controls the flux of turbidites to the deep sea: in principle, sea-level highstands favour the accumulation of sediments on the shelf, whereas sea-level lowstands are expected to result in important sedimentary remobilization and transport towards the deeper parts of aprons (Carey and Schneider, 2011). According to cores in Figures 8 and 10 of Hunt et al. (2013), there are 9 volcanoclastic turbidites originated at Madeira and/or Desertas between 34 ka and 106 ka, which gives a recurrence time of 8 kyrs for large turbidite emplacement. Given the age uncertainties and that turbidites were emplaced during interglacial (MIS 5) and glacial (MIS 3 and 4) periods (when sea-level rose and fell), a correlation between higher productivity of turbidites related to glacio-isostatic changes is impossible to establish.

The islands composing Madeira Archipelago are markedly different concerning their age, subaerial height and morphology, and precipitation rates. Madeira is a young and tall island (almost 2000 m), with extremely incised and high gradient streams, precipitation values up to 3000 mm/year and a known history of flash-floods. These characteristics contrast greatly with the low islands of Porto Santo and Desertas, which feature poorly developed streams, low precipitation rates and did not experience recent volcanism. Unfortunately additional studies presenting high resolution submarine data of tributary systems like these at Madeira Archipelago and at Réunion Island (Mazuel et al., 2016) do not exist, precluding a better discussion on the factors controlling the size of the submarine tributary systems. Nevertheless, some inferences can be drawn based on the diverse islands at Madeira Archipelago. The size of the respective submarine tributary system is apparently controlled by the relatively age of the islands' subaerial topography, and their precipitation rates. Turbidites derived directly from volcanic eruptions are unlikely in Madeira Island because volcanism is dominantly effusive (Geldmacher et al., 2000; Brum da Silveira et al., 2010a). Thus, during flash-floods in Madeira, sediments have probably reached the edge of the shelf as hyperpycnal flows, feeding the gullies and promoting their development. Unfortunately, with exception of the 2010 flash-flood episode, there are no records of sediment concentrations and discharge from streams at Madeira Archipelago. The same process is inferred to explain the well-developed volcani-

clastic deep-sea fans around Réunion Island (Sisavath et al., 2012; Babonneau et al., 2013; Mazuel et al., 2016). These are larger (100–300 km long) than those of Madeira Island because Réunion is taller (~3000 m), subjected to heavier rainfall (>5000 mm/year), and exposed to tropical cyclones. On the older Porto Santo and Desertas islands, which do not exhibit well-developed onshore drainage networks, storm-induced offshore currents were likely the only process delivering sediments to the upper slopes. Such mechanism possibly explains the triggering of small-scale mass-wasting at the shelf edge at Oahu (Tsutsui et al., 1987) and in the Azores (Quartau et al., 2012; Meireles et al., 2013). Data acquisition of shelf currents and river discharge is fundamental to support these inferences and therefore further research is needed to fully understand a possible relationship between stream sediment discharge (and consequently the maturity of drainage networks) and shelf sediment dynamics.

The submarine drainage in Madeira Archipelago is also present on top of debris flow fields, being more developed where these fields are larger. This is because collapse scars commonly act as traps for subsequent sedimentation, leading to enhanced sedimentation rates and increasing the risk of further landslides at the shelf edge (Masson et al., 2006).

5.3. Sediment wave fields

Wave-like features were only found East of Desertas, SE and NE of Porto Santo and NNW of Madeira (Fig. 7). They can be classified into three main types according to their setting: (1) wave fields associated to depositional lobes as in the cases of the major landslides of NNW Madeira, E of Desertas, and SE and NE of Porto Santo; (2) wave fields downstream of the gullies and channels system E of Desertas and; (3) wave fields inside channels, N of Porto Santo (indicated by arrows in Fig. 7). These bedforms generally have wave heights over 9 m (and up to 94 m) and wave lengths exceeding 600 m (and up to 4000 m).

Undulated bedforms are normally generated by bottom currents, either from downslope-flowing turbidity currents or from alongslope-flowing currents (Wynn and Stow, 2002). They can also be formed by soft sediment deformation (e.g. extensional faults or creep folds, Wynn and Stow, 2002). Most of these bedforms occur seaward of the large landslides and are could be compressional features of their debris avalanche deposits, forming poorly-defined depositional distal lobes. In order to distinguish the processes involved in bedform formation, high-resolution seismic reflection and bathymetric data as well as sediment sampling would be required (Wynn and Stow, 2002). However, only high-resolution bathymetry is available for this study, which precludes an interpretation of the wave-forming process. Nevertheless, bedforms with these characteristics (over 6 m height and 300 m wave lengths) are considered large sediment waves, typically located in relatively unconfined settings and composed of fine-grained sediment (Symons et al., 2016). In Madeira Archipelago these features share common characteristics; (1) they occur within the same depth range (3000–4300 m); (2) their crest-lines are always roughly perpendicular to the maximum slope direction; (3) most of them are located where the channel systems end; and, (4) they are located where the seafloor gradients significantly decrease to 0.5° – 3° . Thus, the wave fields were probably generated at the base of the island flanks by deeper unconfined turbidity currents. In addition, the sinuous morphologies are normally found on bedforms generated by flows rather than slope failures (Wynn and Stow, 2002; Symons et al., 2016). These flows were probably initially constrained within the gullies and channels but rapidly became unconfined downslope where the drainage systems open, spreading out over wide areas. Where channel systems are well developed, the flows are confined, and sediment waves do not form

(e.g., N and S of Madeira). Wave fields with similar characteristics (wave height and lengths) have been found in other volcanic environments such as the Aeolian (Casalbore et al., 2014), Canaries (Wynn et al., 2000a), Cape Verde (Masson et al., 2008), Selvagens (Wynn et al., 2000b), and Reunion islands (Mazuel et al., 2016), and were mostly interpreted to have a similar origin. Bedforms with such wave heights and wave lengths are believed to be the result of cyclic steps formed by turbidity currents. Deposition occurs predominantly on the upslope flank and erosion on the downslope flank, resulting in the up-current migration of the bedform crests (Cartigny et al., 2011). The great reduction of slope gradients at –3000 to –4300 m would probably force the flow to pass the hydraulic jump, during which its velocity would be reduced significantly and deposition would occur, favouring the development of these bedforms. Other wave fields found in the South Sandwich (Leat et al., 2010) and Bismarck volcanic arcs (Hoffmann et al., 2008, 2011) were interpreted as formed by both mechanisms (turbidity currents and seafloor deformation). Thus, our preference for the turbidite hypothesis is not strongly supported at this stage without further data.

5.4. Scours

All these features occur within the same depth range (3000–4300 m) and seafloor gradients (0.5° – 3°). There are however some differences in their setting. East of Desertas they are located immediately downslope of the channel systems and upslope of the sediment wave fields. Around Porto Santo they normally lay downslope of the channel systems. Given that the sediment wave fields are hypothesized to be formed by hydraulic jumps driven by significant reduction of seafloor gradients, it is likely that the scours have a similar origin. Unconfined turbidity currents suffer the first significant hydraulic jump due to the reduction of slope gradients, promoting erosion of the seafloor sediment cover (Mutti and Normark, 1987). The downslope sequence of scour and wave fields is common in turbidite systems at continental margins. This sequence normally occurs in the channel-lobe transition zone where a significant reduction of gradients occurs (Wynn et al., 2002). Scours were also found W, SW, and S of Madeira where no channels exist or in ridges between channels. These are normally the largest scours, suggesting that in places where the turbidity currents have no constrain upslope, they have a higher erosive power. Similar features have been found in other volcanic environments such as the Bismarck volcanic arc (Hoffmann et al., 2011), South Sandwich volcanic arc (Leat et al., 2010) and Reunion islands (Saint-Ange et al., 2013) where they are also attributed to the action of unconfined turbidity currents.

6. Conclusions

Once built, the submarine flanks of volcanic ocean islands are shaped by a variety of physical processes that leads to the establishment of large submarine tributary systems that extend to the abyssal plains. These gravitational, erosional, and depositional processes, however, are still poorly understood, and so are many of the morphologies associated to such tributary systems. In particular, it is still not clear how distinct morpho-climatic conditions of individual volcanic islands influence erosion and deposition in their submarine environments. To address this problem, we performed a comprehensive overlook at the gravitational, erosional, and depositional processes affecting the submarine flanks of an entire archipelago, using a high-resolution dataset covering from the nearshore to the abyssal plains. This study is therefore one of the few to offer a comprehensive source-to-sink approach in the study of submarine tributary systems, linking different island subaerial

morphologies and physiographic conditions with near-shore shelf, slope, and far-field abyssal features. Additionally to being the first morphological description of the seafloor around Madeira, Porto Santo, and Desertas Islands, this study allowed a comparison with other archipelagos, showing how distinct island characteristics promote diverse submarine evolutions.

Especially outstanding is the finding of landslide scars and respective deposits produced by huge subaerial and submarine flank collapses, with dimensions comparable to some of the large landslides in Hawaii or the Canary Islands. As proposed to other archipelagos, a clear relationship between island size and landslide areas was shown to exist, but an obvious link between island height and landslide areas proved more elusive. The integration of the subaerial and submarine data also allowed a discussion of their ages, pointing at least to kyrs to a few Myrs.

A widespread submarine tributary system that initiates at the shelf edge of the islands revealed how sediments are dislodged and transported downslope to form volcanoclastic aprons. At Madeira Island, sediments reached the shelf edge by hyperpycnal flows to induce mass-wasting, showing the importance of such process on highly-dissected edifices subjected to high riverine discharge, as it also happens in Réunion Island. In Desertas and Porto Santo, sediments were more likely transported offshore during storms. Some of these tributary systems develop on top of the large landslide scars and paths reinforcing that these slides are older features.

The presence of scours and sediment waves show that, as sediments reach the lower slopes of the islands, the sudden gradient decrease promotes hydraulic jumps that first, causes the formation of scours, and second, of wave fields. Sediment waves appear mostly in the depositional lobes of the landslides and seaward of poorly-developed channel systems. Where channel systems are well developed and/or protruding rocky outcrops exist, sediment wave fields are absent. The largest scours are only present in areas without channel systems, showing that in these places the hydraulic jump produced by upslope unconstrained turbidite currents is enhanced. Our data strongly supports the general conclusion that high and rainy islands tend to form well-developed and confined volcanoclastic turbidite systems, whilst on low and dry islands unconfined and smaller turbidite systems predominate, favouring the development of scours and sediment wave fields.

Acknowledgements

This work is a contribution of SEDMAR program funded by IH. EMEPC and IFREMER are acknowledged for sharing datasets (respectively multibeam bathymetry and multichannel seismic reflection profiles). RQ and RR acknowledge their IF/00635/2015 and IF/01641/2015 contracts funded by Fundação para a Ciência e a Tecnologia. Duarte Costa at Direção de Serviços de Informação Geográfica e Cadastro do Governo Regional da Madeira is acknowledged for providing the digital altimetry used in this study. Neil Mitchell, an anonymous reviewer and the Editor Tamsin Mather are gratefully acknowledged for suggestions that significantly improved this manuscript.

Appendix A. Supplementary material

Supplementary material related to this article can be found online at <https://doi.org/10.1016/j.epsl.2017.11.003>.

References

Acosta, J., Uchupi, E., Muñoz, A., Herranz, P., Palomo, C., Ballesteros, M., 2003. Geologic evolution of the Canarian Islands of Lanzarote, Fuerteventura, Gran Canaria and La Gomera and comparison of landslides at these islands with those at Tenerife, La Palma and El Hierro. *Mar. Geophys. Res.* 24, 1–40.

- Babonneau, N., Delacourt, C., Cancouët, R., Sisavath, E., Bachèlery, P., Mazuel, A., Jorry, S.J., Deschamps, A., Ammann, J., Villeneuve, N., 2013. Direct sediment transfer from land to deep-sea: insights into shallow multibeam bathymetry at La Réunion Island. *Mar. Geol.* 346, 47–57.
- Baioni, D., 2011. Human activity and damaging landslides and floods on Madeira Island. *Nat. Hazards Earth Syst. Sci.* 11, 3035–3046.
- Brum da Silveira, A., Madeira, J., Ramalho, R., Fonseca, P., Prada, S., 2010a. Notícia Explicativa da Carta Geológica da Ilha da Madeira na Escala 1:50.000, Folhas A e B. Secretaria Regional do Ambiente e Recursos Naturais e Universidade da Madeira. ISBN 978-972-98405-2-4. 47 p.
- Brum da Silveira, A., Madeira, J., Ramalho, R., Fonseca, P., Rodrigues, C., Prada, S., 2010b. Carta Geológica da Ilha da Madeira na Escala 1:50.000, Folhas A e B. Secretaria Regional do Ambiente e Recursos Naturais e Universidade da Madeira. ISBN 978-972-98405-1-7. 2 sheets at the 1:50,000 scale.
- Calder, B.R., Mayer, L.A., 2003. Automatic processing of high-rate, high-density multibeam echosounder data. *Geochem. Geophys. Geosyst.* 4.
- Carey, S.N., Schneider, J.-L., 2011. Chapter 7 – Volcaniclastic processes and deposits in the deep-sea. In: Heiko, H., Thierry, M. (Eds.), *Developments in Sedimentology*. Elsevier, Amsterdam, pp. 457–515.
- Cartigny, M.J.B., Postma, G., van den Berg, J.H., Mastbergen, D.R., 2011. A comparative study of sediment waves and cyclic steps based on geometries, internal structures and numerical modeling. *Mar. Geol.* 280, 40–56.
- Casalbore, D., Romagnoli, C., Bosman, A., Chiocci, F.L., 2014. Large-scale seafloor waveforms on the flanks of insular volcanoes (Aeolian Archipelago, Italy), with inferences about their origin. *Mar. Geol.* 355, 318–329.
- Cornen, G., Girardeau, J., Agrinier, P., Grasset, O., Hinscherberger, F., Loyer, H., Malod, J., Matias, L., Monteiro, L., Pinheiro, J., Quilacq, B.D., Ribeiro, A., Thionin, I., 2003. Campagne Tore-Madère – Premiers Résultats. Rapport non publié, Univ-Nantes, p. 113.
- Ferreira, J.C., Cunha, L.V., 1984. Prediction of Soil Erosion in the Island of Porto Santo (Portugal). *Memória LNEC* 622, Lisboa.
- Geldmacher, J., Hoernle, K., Klügel, A., van den Bogaard, P., Duggen, S., 2006. A geochemical transect across a heterogeneous mantle upwelling: implications for the evolution of the Madeira hotspot in space and time. *Lithos* 90, 131–144.
- Geldmacher, J., van den Bogaard, P., Hoernle, K., Schmincke, H.-U., 2000. The 40Ar/39Ar age dating of the Madeira Archipelago and hotspot track (eastern North Atlantic). *Geochem. Geophys. Geosyst.* 1, 1–26.
- Hoffmann, G., Silver, E., Day, S., Morgan, E., Driscoll, N., Orange, D., 2008. Sediment waves in the Bismarck Volcanic Arc, Papua New Guinea. *Spec. Pap., Geol. Soc. Am.* 436, 91–126.
- Hoffmann, G., Silver, E., Day, S.J., Driscoll, N., Orange, D., 2011. Deformation versus deposition of sediment waves in the Bismarck Sea, Papua New Guinea. In: Shipp, R.C., Weimer, P., Posamentier, H.W. (Eds.), *Mass-Transport Deposits in Deepwater Settings*. SEPM Society for Sedimentary Geology, Tulsa, pp. 455–474.
- Hunt, J.E., Talling, P.J., Clare, M.A., Jarvis, I., Wynn, R.B., 2014. Long-term (17 Ma) turbidite record of the timing and frequency of large flank collapses of the Canary Islands. *Geochem. Geophys. Geosyst.* 15, 3322–3345.
- Hunt, J.E., Wynn, R.B., Talling, P.J., Masson, D.G., 2013. Frequency and timing of landslide-triggered turbidity currents within the Agadir Basin, offshore NW Africa: are there associations with climate change, sea level change and slope sedimentation rates? *Mar. Geol.* 346, 274–291.
- Klügel, A., Klein, F., 2006. Complex magma storage and ascent at embryonic submarine volcanoes from the Madeira Archipelago. *Geology* 34, 337–340.
- Klügel, A., Schwarz, S., van den Bogaard, P., Hoernle, K., Wohlgemuth-Ueberwasser, C., Köster, J., 2009. Structure and evolution of the volcanic rift zone at Ponta de São Lourenço, eastern Madeira. *Bull. Volcanol.* 71, 671–685.
- Krastel, S., Schmincke, H.-U., Jacobs, C.L., 2001. Formation of submarine canyons on the flanks of the Canary Islands. *Geo Mar. Lett.* 20, 160–167.
- Leat, P.T., Tate, A.J., Tappin, D.R., Day, S.J., Owen, M.J., 2010. Growth and mass wasting of volcanic centers in the northern South Sandwich arc, South Atlantic, revealed by new multibeam mapping. *Mar. Geol.* 275, 110–126.
- Lira, C., Lousada, M., Falcão, A.P., Gonçalves, A.B., Heleno, S., Matias, M., Pereira, M.J., Pina, P., Sousa, A.J., Oliveira, R., Almeida, A.B., 2013. The 20 February 2010 Madeira Island flash-floods: VHR satellite imagery processing in support of landslide inventory and sediment budget assessment. *Nat. Hazards Earth Syst. Sci.* 13, 709–719.
- Llanes, P., Herrera, R., Gómez, M., Muñoz, A., Acosta, J., Uchupi, E., Smith, D., 2009. Geological evolution of the volcanic island La Gomera, Canary Islands, from analysis of its geomorphology. *Mar. Geol.* 264, 123–139.
- Manville, V., Németh, K., Kano, K., 2009. Source to sink: a review of three decades of progress in the understanding of volcanoclastic processes, deposits, and hazards. *Sediment. Geol.* 220, 136–161.
- Masson, D.G., Watts, A.B., Gee, M.J.R., Urgeles, R., Mitchell, N.C., Le Bas, T.P., Canals, M., 2002. Slope failures on the flanks of the western Canary Islands. *Earth-Sci. Rev.* 57, 1–35.
- Masson, D.G., Harbitz, C.B., Wynn, R.B., Pedersen, G., Løvholt, F., 2006. Submarine landslides: processes, triggers and hazard prediction. *Philos. Trans. R. Soc. A* 364, 2009–2039.
- Masson, D.G., Le Bas, T.P., Grevemeyer, I., Weinrebe, W., 2008. Flank collapse and large-scale landsliding in the Cape Verde Islands, off West Africa. *Geochem. Geophys. Geosyst.* 9. <https://doi.org/10.1029/2008GC001983>.

- Mata, J., Fonseca, P., Prada, S., Rodrigues, D., Martins, S., Ramalho, R., Madeira, J., Cachão, M., Marques da Silva, C., Matias, M.J., 2013. O arquipélago da Madeira. In: Dias, R., Araújo, A., Terrinha, P., Kullberg, J.C. (Eds.), *Geologia de Portugal, Volume II – Geologia Meso-cenozóica de Portugal*. Escolar Editora, pp. 691–746.
- Mazuel, A., Sisavath, E., Babonneau, N., Jorry, S.J., Bachèlery, P., Delacourt, C., 2016. Turbidity current activity along the flanks of a volcanic edifice: the Mafate volcanoclastic complex, La Réunion Island, Indian Ocean. *Sediment. Geol.* 335, 34–50.
- Meireles, R., Quartau, R., Ramalho, R.S., Rebelo, A.C., Madeira, J., Zanon, V., Ávila, S.P., 2013. Depositional processes on oceanic island shelves – evidence from storm-generated Neogene deposits from the mid-North Atlantic. *Sedimentology* 60, 1769–1785.
- Mitchell, N.C., 2003. Susceptibility of mid-ocean ridge volcanic islands and seamounts to large-scale landsliding. *J. Geophys. Res.* 108, 2397. B8.
- Mitchell, N.C., Dade, W.B., Masson, D.G., 2003. Erosion of the submarine flanks of the Canary Islands. *J. Geophys. Res.* 108, 3–1–3–11.
- Moore, J.G., Clague, D.A., Holcomb, R.T., Lipman, P.W., Normark, W.R., Torresan, M.E., 1989. Prodigious submarine landslides on the Hawaiian Ridge. *J. Geophys. Res., Solid Earth* 94, 17465–17484.
- Mutti, E., Normark, W.R., 1987. Comparing examples of modern and ancient turbidite systems: problems and concepts. In: Leggett, J.K., Zuffa, G.G. (Eds.), *Marine Clastic Sedimentology: Concepts and Case Studies*. Graham and Trotman, London, pp. 1–38.
- Paris, R., Ramalho, R.S., Madeira, J., Ávila, S., May, S.M., Rixhon, G., Engel, M., Brückner, H., Herzog, M., Schukraft, G., Perez-Torrado, F.J., Rodriguez-Gonzalez, A., Carracedo, J.C., Giachetti, T., 2018. Mega-tsunami conglomerates and flank collapses of ocean island volcanoes. *Mar. Geol.* 395, 168–187.
- Piper, D.J.W., Normark, W.R., 2009. Processes that initiate turbidity currents and their influence on turbidites: a marine geology perspective. *J. Sediment. Res.* 79, 347–362.
- Prada, S.N., Silva, M.O., Cruz, J.V., 2005. Groundwater behaviour in Madeira, volcanic island (Portugal). *Hydrogeol. J.* 13, 800–812.
- Quartau, R., Mitchell, N.C., 2013. Comment on “Reconstructing the architectural evolution of volcanic islands from combined K/Ar, morphologic, tectonic, and magnetic data: the Faial Island example (Azores)” by Hildenbrand et al. (2012) [*J. Volcanol. Geotherm. Res.* 241–242 (2012) 39–48]. *J. Volcanol. Geotherm. Res.* 255, 124–126.
- Quartau, R., Trenhaile, A.S., Mitchell, N.C., Tempera, F., 2010. Development of volcanic insular shelves: insights from observations and modelling of Faial Island in the Azores Archipelago. *Mar. Geol.* 275, 66–83.
- Quartau, R., Tempera, F., Mitchell, N.C., Pinheiro, L.M., Duarte, H., Brito, P.O., Bates, R., Monteiro, J.H., 2012. Morphology of the Faial Island shelf (Azores): the interplay between volcanic, erosional, depositional, tectonic and mass-wasting processes. *Geochem. Geophys. Geosyst.* 13, Q04012. <https://doi.org/10.1029/2011GC003987>.
- Quartau, R., Hipólito, A., Romagnoli, C., Casalbone, D., Madeira, J., Tempera, F., Roque, C., Chiocci, F.L., 2014. The morphology of insular shelves as a key for understanding the geological evolution of volcanic islands: insights from Terceira Island (Azores). *Geochem. Geophys. Geosyst.* 15, 1801–1826.
- Quartau, R., Hipólito, A., Mitchell, N.C., Gaspar, J.L., Brandão, F., 2015a. Comment on “Construction and destruction of a volcanic island developed inside an oceanic rift: Graciosa Island, Terceira Rift, Azores” by Sibrant et al. (2014) and proposal of a new model for Graciosa geological evolution [*J. Volcanol. Geotherm. Res.* 284 (2014) 32–45]. *J. Volcanol. Geotherm. Res.* 303, 146–156.
- Quartau, R., Madeira, J., Mitchell, N.C., Tempera, F., Silva, P.F., Brandão, F., 2015b. The insular shelves of the Faial-Pico Ridge: a morphological record of its geologic evolution (Azores archipelago). *Geochem. Geophys. Geosyst.* 16, 1401–1420.
- Quartau, R., Madeira, J., Mitchell, N.C., Tempera, F., Silva, P.F., Brandão, F., 2016. Reply to comment by Marques et al. on “The insular shelves of the Faial-Pico Ridge (Azores archipelago): a morphological record of its evolution”. *Geochem. Geophys. Geosyst.* 17, 633–641.
- Ramalho, R.S., Brum da Silveira, A., Fonseca, P., Madeira, J., Cosca, M., Cachão, M., Fonseca, M., Prada, S., 2015. The emergence of volcanic oceanic islands on a slow-moving plate: the example of Madeira Island, NE Atlantic. *Geochem. Geophys. Geosyst.* 16, 522–537.
- Saint-Ange, F., Bachèlery, P., Babonneau, N., Michon, L., Jorry, S.J., 2013. Volcaniclastic sedimentation on the submarine slopes of a basaltic hotspot volcano: piton de la Fournaise volcano (La Réunion Island, Indian Ocean). *Mar. Geol.* 337, 35–52.
- Schmidt, R., Schmincke, H.-U., 2002. From seamount to oceanic island, Porto Santo, central East-Atlantic. *Int. J. Earth Sci. (Geol. Rundsch.)* 91, 594–614.
- Schmincke, H.-U., Sumita, M., 1998. Volcanic evolution of Gran Canaria reconstruction from apron sediments: synthesis of VICAP project drilling. In: Weaver, P.P.E., Schmincke, H.-U., Firth, J.V., Duffield, W. (Eds.), *Proc. Ocean Drill. Prog. Sci. Res.*, vol. 157, pp. 443–469.
- Schwarz, S., Klügel, A., van den Bogaard, P., Geldmacher, J., 2005. Internal structure and evolution of a volcanic rift system in the eastern North Atlantic: the Desertas rift zone, Madeira archipelago. *J. Volcanol. Geotherm. Res.* 141, 123–155.
- Siebert, L., 1984. Large volcanic debris avalanches: characteristics of source areas, deposits, and associated eruptions. *J. Volcanol. Geotherm. Res.* 22, 163–197.
- Sisavath, E., Babonneau, N., Saint-Ange, F., Bachèlery, P., Jorry, S.J., Deplus, C., De Voogd, B.A., Savoye, B., 2011. Morphology and sedimentary architecture of a modern volcanoclastic turbidite system: the Cilaos fan, offshore La Réunion Island. *Mar. Geol.* 288, 1–17.
- Sisavath, E., Mazuel, A., Jorry, S.J., Babonneau, N., Bachèlery, P., de Voogd, B., Salpin, M., Emmanuel, L., Beaufort, L., Toucanne, S., 2012. Processes controlling a volcanoclastic turbiditic system during the last climatic cycle: example of the Cilaos deep-sea fan, offshore La Réunion Island. *Sediment. Geol.* 281, 180–193.
- Symons, W.O., Sumner, E.J., Talling, P.J., Cartigny, M.J.B., Clare, M.A., 2016. Large-scale sediment waves and scours on the modern seafloor and their implications for the prevalence of supercritical flows. *Mar. Geol.* 371, 130–148.
- Tsutsui, B., Campbell, J.F., Coulbourn, W.T., 1987. Storm-generated, episodic sediment movements off Kahe Point, Oahu, Hawaii. *Mar. Geol.* 76, 281–299.
- Wynn, R.B., Kenyon, N.H., Masson, D.G., Stow, D.A.V., Weaver, P.P.E., 2002. Characterization and recognition of deep-water channel-lobe transition zones. *AAPG Bull.* 86, 1441–1462.
- Wynn, R.B., Masson, D.G., Stow, D.A.V., Weaver, P.P.E., 2000a. Turbidity current sediment waves on the submarine slopes of the western Canary Islands. *Mar. Geol.* 163, 185–198.
- Wynn, R.B., Stow, D.A.V., 2002. Classification and characterization of deep-water sediment waves. *Mar. Geol.* 192, 7–22.
- Wynn, R.B., Weaver, P.P.E., Ercilla, G., Stow, D.A.V., Masson, D.G., 2000b. Sedimentary processes in the Selvage sediment-wave field, NE Atlantic: new insights into the information of sediment waves by turbidity currents. *Sedimentology* 47, 1181–1197.